SPECTRAL CHARACTERIZATION OF MARTIAN SOIL ANALOGUES

David G. Agresti, Ph. D.
Associate Professor of Physics
University of Alabama at Birmingham
Birmingham, AL 35294

ABSTRACT

As reported by Dr. Richard Morris in March, reflectance spectra of iron (III) oxide precipitated as ultrafine (x-ray amorphous) particles, unlike ordinary fine-grained (>100 nm) hematite (α-Fe_2O_3), have significant similarities to reflectance spectra from the bright regions of Mars. During this summer's stay at JSC, I have collaborated with Dr. Morris to characterize these particles according to composition, magnetic properties, and particle-size distribution. Mossbauer, magnetic susceptibility, and optical data have been obtained for samples with a range of concentrations of iron oxide in silica gel of varying pore diameters (6, 15, and 30 nm). To analyze the Mossbauer spectra, I have enhanced a versatile fitting program (adapted during last summer's ASEE visit for the IBM-PC) to provide user-friendly screen input and theoretical models appropriate for the superparamagnetic spectra obtained.

NASA Colleague: Richard V. Morris, Ph. D., SN4, X5874

INTRODUCTION

In March of this year [Morris and Lauer, 1986], Dr. Richard Morris reported that hematite formed by calcining silica gel impregnated with ferric nitrate solution provided a material with spectra similar to reflectance spectra obtained from the bright regions of Mars. The hematite has an ultrafine particle size because of the small pore size (6-30 nm) of the silica gel matrix in which it is prepared. Further work in Dr. Morris' laboratory at JSC has been aimed at producing a variety of samples of this material in gels of various pore sizes and under varying conditions of temperature of oxidation, pH, starting reagents, etc., in order to produce the material with the best match to the Mars spectrum. Other techniques are employed to further characterize the properties of these martian soil analogues and to determine the magnetic properties, chemical composition, size distribution, etc., of the particles of which this material is made.

One of the tools employed by Dr. Morris in this effort is Mossbauer spectroscopy. In this technique, a spectrum is obtained by allowing radiation emitted from a moving source of 14.4-keV gamma-rays from ^{57}Fe (about 2% of natural iron) to pass through the material (absorber) under study. This transmission spectrum is obtained in a multichannel analyzer as a plot of number of gamma-ray counts detected versus the

velocity of the source (1 mm/s corresponds to an energy shift of 4.8×10^{-8} eV) [for example, Figure 1]. The spectrum is analyzed by computer fitting a theoretical function to the data and interpreting the fitted parameters in terms of the environment of the iron atoms in the absorber material.

In the present study, spectra generally consist of a 6-peak magnetic spectrum superimposed on a 2-peak paramagnetic spectrum [Figure 2]. The simplest interpretation of the spectra observed is that the iron atoms are in two chemically distinct sites, one of which results in a magnetic field at the iron nucleus. However, it is well-known that iron oxide particles < 30nm in diameter exhibit superparamagnetism [Kundig et al., 1966]. In this report, the phenomenon of superparamagnetism will be discussed and applied to the silica-gel oxides to obtain useful information about the particle-size distribution in these samples.

In continuing with the adaptation for the IBM-PC of the Mossbauer data least-squares fitting program [Agresti et al., 1969] begun last summer [Agresti, 1985], I have attempted to provide a more user-friendly screen input and fitting models particularly suited to the Mossbauer spectra obtained on the martian soil analogues. In this report, several of these enhancements will be described and illustrated by application to spectra obtained in Dr. Morris' laboratory.

SUPERPARAMAGNETISM

As stated in the introduction, iron oxide formed in silica gel may be superparamagnetic. The samples obtained generally have Mossbauer spectra with a 6-peak magnetic component, which implies the presence of a magnetic field at the nucleus (31.15 kOe per mm/s of splitting between the outer pair of lines), and a 2-peak paramagnetic component, which implies the absence of a magnetic field, or more properly, a zero time-average magnetic field. The 2-peak splitting results from the distortion of the local environment of the iron atom from cubic symmetry. Superparamagnetic particles are so small that the magnetic anisotropy energy, which is proportional to volume, is not sufficient to maintain the domain magnetization pointing permanently in one of several possible easy directions in the crystal, and the magnetizetion flips among easy directions with a frequency related to the thermal energy, kT. The reciprocal of this frequency, the relaxation time, t_o, is proportional to the Maxwell-Boltzmann weighting factor:

$$t_o \propto \exp(2KV/kT), \qquad (1)$$

where K is the magnetic anisotropy constant and V is the volume of the superparamagnetic particle.

In order for a magnetic field to be observed at the nucleus (resulting in a 6-line pattern), t_o must be long compared to the time of observation, t_{obs}; a 2-line pattern

will appear when t_o is much shorter than t_{obs}. The time, t_{obs}, is necessary to establish the value of the field at the nucleus, and, from the Heisenberg uncertainty product, is equal to the nuclear level splitting resulting from the magnetic field divided by Planck's constant, $\hbar$. (For the 500 kOe fields of α-Fe_2O_3, t_{obs} is approx. equal to 2.5×10^{-8} sec). Thus, from the spectrum shown in Figure 2, our sample consists of a distribution of particle sizes, the smaller particles being associated with the doublet and the larger particles with the sextet. The area under each of these two components of the spectrum is proportional to the number of nuclei, that is, the total volume, in each size regime.

To obtain a size distribution, and also to confirm the supermagnetic nature of our samples, it is necessary to collect Mossbauer spectra over a range of temperatures. Figure 3 shows a series of Mossbauer spectra collected down to 22K on a silica gel sample supplied by Dr. Morris. These were taken by my graduate student and NASA Graduate Trainee Jeffrey Newcomb at UAB. In the figure, it is seen that there is a steady increase with temperature of the 2-peak component at the expense of the 6-peak component.

To explain this effect, we point out that Equation (1) shows that t_o depends on temperature as well as on particle size. In fact, the exponential dependence implies a fairly sharp transition as a function of temperature, for a given particle volume V, between a 6-peak and a 2-peak contribution

to the spectrum. From another point of view, for each temperature there is a transitional volume, V_t, that divides the distribution into two parts. For $V > V_t$, the particles contribute to the 6-peak component; for $V < V_t$, to the 2-peak component. Kundig et al. determined that the anisotropy constant, K, for hematite is approximately independent of temperature and gave a value of $(4.1 \pm 1) \times 10^4$ erg/cm^3. With this value and the requirement that the relaxation time, t_o, for particles of volume, V_t, be approx. = t_{obs}, Equation (1) may be transformed [from Eq. (8), Kundig et al., 1966] to the more convenient form,

$$V_t = [(4.7 \pm 1)\ \text{nm}^3]\ T. \qquad (2)$$

The spectra of Figure 3 were fit to determine the relative area of the 2-peak component. Figure 4 is a graph of the results with a smooth curve drawn through the data. The curve may be understood to be proportional to the integral of the distribution, dN(T)/dV, which is the number of particles having volume in the range between V_t and V_t+dV, since this integral from zero K to the temperature, T, is equal to the total volume of particles with $V < V_t$. Hence, the derivative of the curve, under the assumption of constant K, gives directly a volume distribution, which may be calibrated according to Equation (2). This distribution may be converted into the desired size distribution if we assume the particles are uniform spheres, as has been done in Figure 4.

THE COMPUTER PROGRAM

The major portion of my effort this summer was devoted to enhancing the computer program [Agresti et al., 1969] used to analyze the Mossbauer data. The resulting program, along with future enhancements, will be designated "VersiFit." Last summer, the program was implemented on an IBM-PC, but, as mentioned then [Agresti, 1985], a number of modifications remained to be made. Five such enhancements will be described here in order to illustrate the range of modifications involved: These are: 1. Interactive screen input; 2. Plotting of data and fitted function; 3. Laser velocity calibration; 4. Marquardt minimization procedure; and 5. Skewed-Lorentzian peak functions.

1. Interactive screen input. Sample input screens are shown in Figure 5. Other input screens are provided or anticipated for input of relations among parameters, data and velocity definition, plotting requirements, etc. The basic idea is a complete break with the fixed-sequence input typical of mainframe computers. It is not only interactive, but dynamic in the sense that the user decides which information to provide through the use of the cursor controls to position the response in the correct box and through the selection of particular entry screens that contain the items required. Furthermore, the individual entry screens re-form themselves in response to earlier input, as shown by the

three screens of Figure 5. It is hoped that this more user-friendly type of input coupled with implementation on a very popular and very powerful microcomputer will ease the adoption of the program among the mineralogical community.

2. Plotting of data and fitted function. The PC used this summer is configured with a graphics printer, a monochrome monitor used for text and numerical input and output, and a high-resolution (640x200) graphics monitor used to display graphs of data and fitted function. This arrangement has proved very helpful when analyzing data. The visual display of data and function on the same graph [Figures 6,11,12] is of course much more helpful for inspecting the quality of the fit than merely noting, for example, the value of chi square (χ^2). But it is also useful for making good choices for starting values of parameters in the fit, as are plots of deviations between data and function [Figures 7,8]. With a graphics printer connected, immediate hard-copy output may be obtained for later reference or publication.

3. Laser velocity calibration. As described in the introduction, the spectrum is acquired in a multichannel analyzer with a moving source of radiation. The drive produces a velocity designed to be linearly proportional to channel number; thus, $v_i = m \times (i - 256.5)$, where m = velocity increment (mm/s) per channel and i ranges from 1 to 512, the number of channels. In order to obtain a precise

value for the velocity of the source, a laser is mounted parallel with the motion of the source and interference fringes are counted and stored as a function of channel. The number of fringes produced is accurately proportional to the distance covered during the period of time a channel is open, hence to the absolute value of the velocity. Figure 9 is a typical laser calibration run, associated with the data of Figures 1,2,11,12. The calibration data show that the velocity is not strictly linear, but is better represented by a "bilinear" function, $v_i = m_1 \times (i - i_o)$ for $i < i_o$, and $v_i = m_2 \times (i - i_o)$ for $i > i_o$, where m_1 and m_2 typically differ by 1%, and i_o, which corresponds to the zero-velocity channel, is generally not equal to 256.5.

4. Marquardt minimization procedure. As noted in last summer's report [Agresti, 1985], the standard non-linear least-squares fitting procedure, employing Taylor's approximation for the function, is not always successful in obtaining a minimum in χ^2, defined as

$$\chi^2 = \frac{1}{(N_d - N_p)} \sum \frac{(y_i - f_i)^2}{\sigma_i^2} \qquad (3)$$

where N_d is the number of data values (channels), N_p is the number of parameters varied in the fit, and σ_i is the standard deviation in each data value. When parameters are strongly correlated, as the peak positions of Figure 6, where the peaks strongly overlap, say in fitting with two or three overlapping doublets, then often this procedure will

produce an increasing χ^2 from iteration to iteration. A different approach [Marquardt, 1963] combines steepest descent with Taylor's approximation in such a way that the change in the parameters is neither Taylor nor steepest descent but a linear combination of the two. The linear combination is optimal in that the fit converges to a minimum in the least number of iterations. According to theory, the fit will converge, even when parameters are strongly correlated. To illustrate this, Figure 10 shows the variation in χ^2 for 6-peak fits to the data of Figure 6 with two sets of starting parameters and minimization by the Taylor or Marquardt procedure. Started close to the minimum in χ^2 of 0.966, Taylor is very sluggish compared to Marquardt; started farther away, it diverges, while Marquardt proceeds monotonically downward.

5. Skewed-Lorentzian peak functions. Figure 1 shows a spectrum of pure, bulk hematite. Each component peak is symmetrical in comparison to those of Figure 2. In order to accurately fit the areas, a satisfactory shape function must be supplied that will successfully reproduce the shape of the data. In the case of hematite and many other particularly well-defined crystal structures, the appropriate theoretical function is a Lorentzian, given by:

$$L(v) = \frac{\text{Area} \times 2 / (\pi W)}{1 + [2 (v - v_o) / W]^2}, \qquad (4)$$

where v_o is the velocity position of the peak (more

accurately, dip) in the transmission spectrum, and W is the full-width at half maximum. Figure 11 shows a fit of the data of Figure 2 to a superposition of 8 Lorentzian peaks, with areas and widths constrained in pairs, resulting in 18 variable parameters. The value achieved for χ^2 is 8.98, and it is easy to see that the fitted function misses a great deal of the data. From the above discussion, it is evident that we must account for the asymmetry in the 6 magnetic peaks. The function I have chosen, for computational simplicity, may be termed a "skewed" Lorentzian. It has an additional parameter, δ, the "skew," and is defined (assuming $\delta > 1$) by contracting the half-width to .5 W / δ on one side of the vertical midline of the Lorentzian function and expanding the width to .5 W x δ on the other side. Figure 12 shows the fitted function obtained with the 6 magnetic peaks skewed in pairs. The final value of χ^2 has dropped to 1.35, a dramatic improvement for the addition of just 3 additional variable parameters.

In summary, improvements in the capabilities for analysis of Mossbauer spectra of martian soil analogues have been provided as a modification of an existing least-squares program, whose ease of input and variety of fitting options and models, hence VersiFit, should be of value to those in the wider scientific community who wish to employ desk-top computers in their data analysis.

ACKNOWLEDGMENTS

I wish to thank NASA and the Summer Faculty Fellowship Program for providing me with the opportunity to spend two very productive summers in a very stimulating environment. Above all, thanks to Dick Morris for much encouragement and many interesting discussions and for exposing me to an application of Mossbauer spectroscopy entirely new to me. We have started a very fine collaboration, and it will continue.

REFERENCES

1. Agresti, D.G., M.F. Bent, and B.I. Persson, "A Versatile Computer Program for Analysis of Mossbauer Spectra," Nucl. Instr. and Methods, Vol. 72, pp. 235-236, 1969.

2. Agresti, D.G., "Mossbauer Spectroscopy of Extraterrestrial Materials," Final Report, NASA/ASEE Summer Faculty Fellowship Program, Summer, 1985.

3. Kundig, W., H. Bommel, G. Constabaris, and R. Lindquist, "Some Propertiesof Supported Small α-Fe_2O_3 Particles Determined with the Mossbauer Effect," Phys. Rev., Vol. 142, pp. 327-333, 1966.

4. Marquardt, D.W., "An Algorithm for Least-Squares Estimation of Nonlinear Parameters," J. Soc. Indust. Appl. Math., Vol. 11, pp. 431-441, 1963.

5. Morris, R.V., and H.V. Lauer, Lunar and Planetary Science Conference XVII Abstracts (Houston, March, 1986), pp. 573-574.

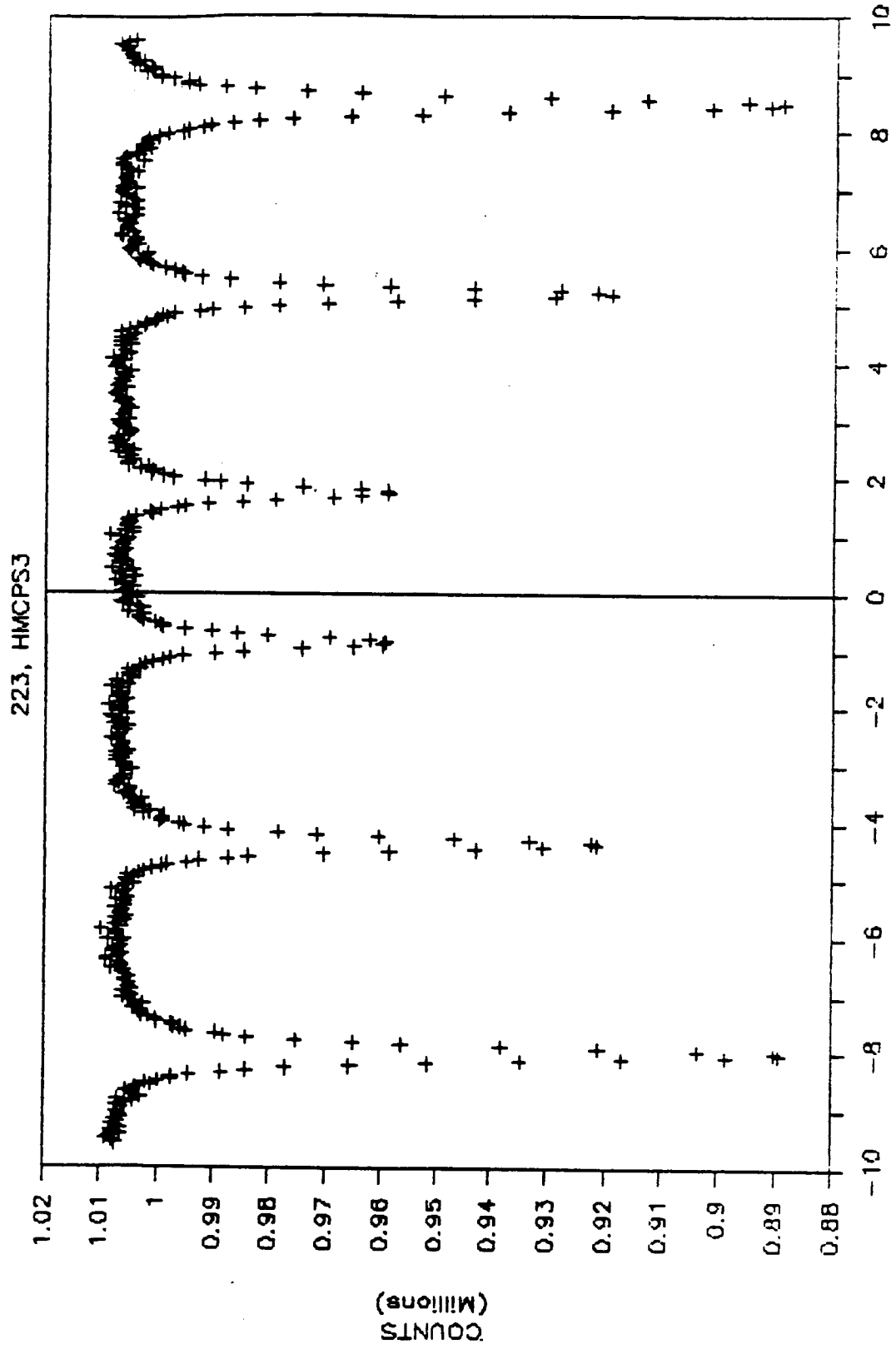

Figure 1. Mossbauer spectrum of bulk hematite.

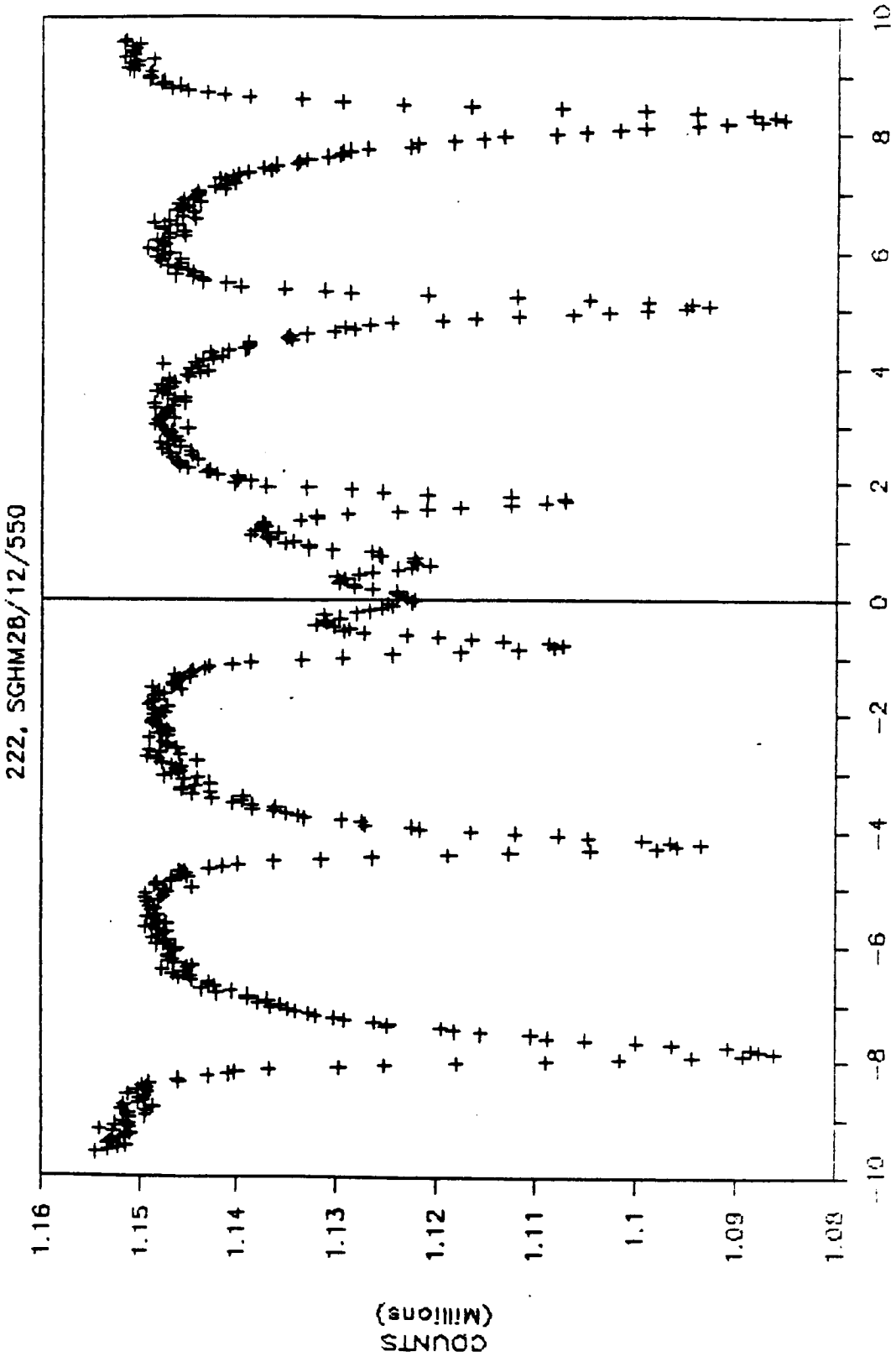

Figure 2. Room temperature Mossbauer spectrum of a sample of Fe_2O_3 (23.7 wt%) in 6-nm silica gel.

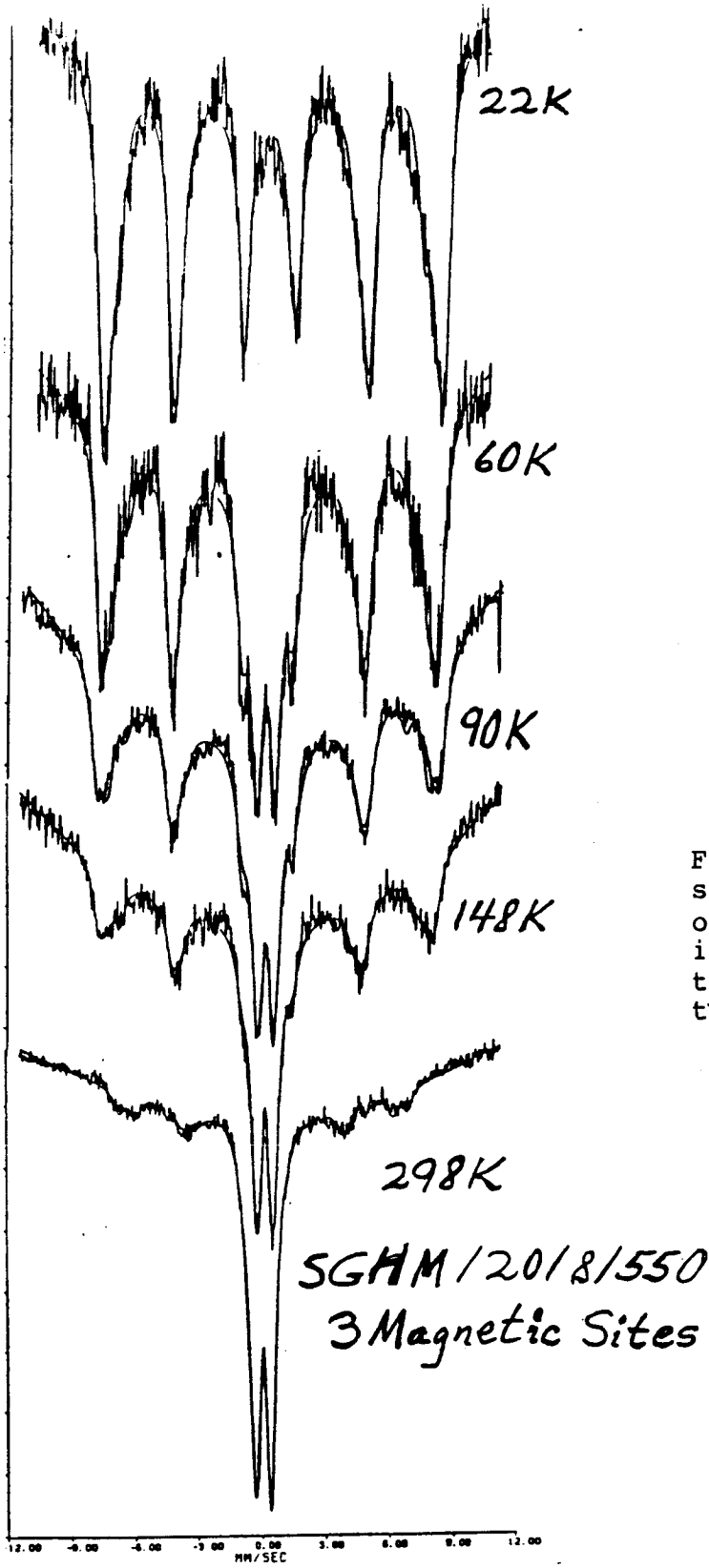

Figure 3. Mossbauer spectra of a sample of Fe_2O_3 (5.73 wt%) in 6-nm silica gel, taken at various temperatures.

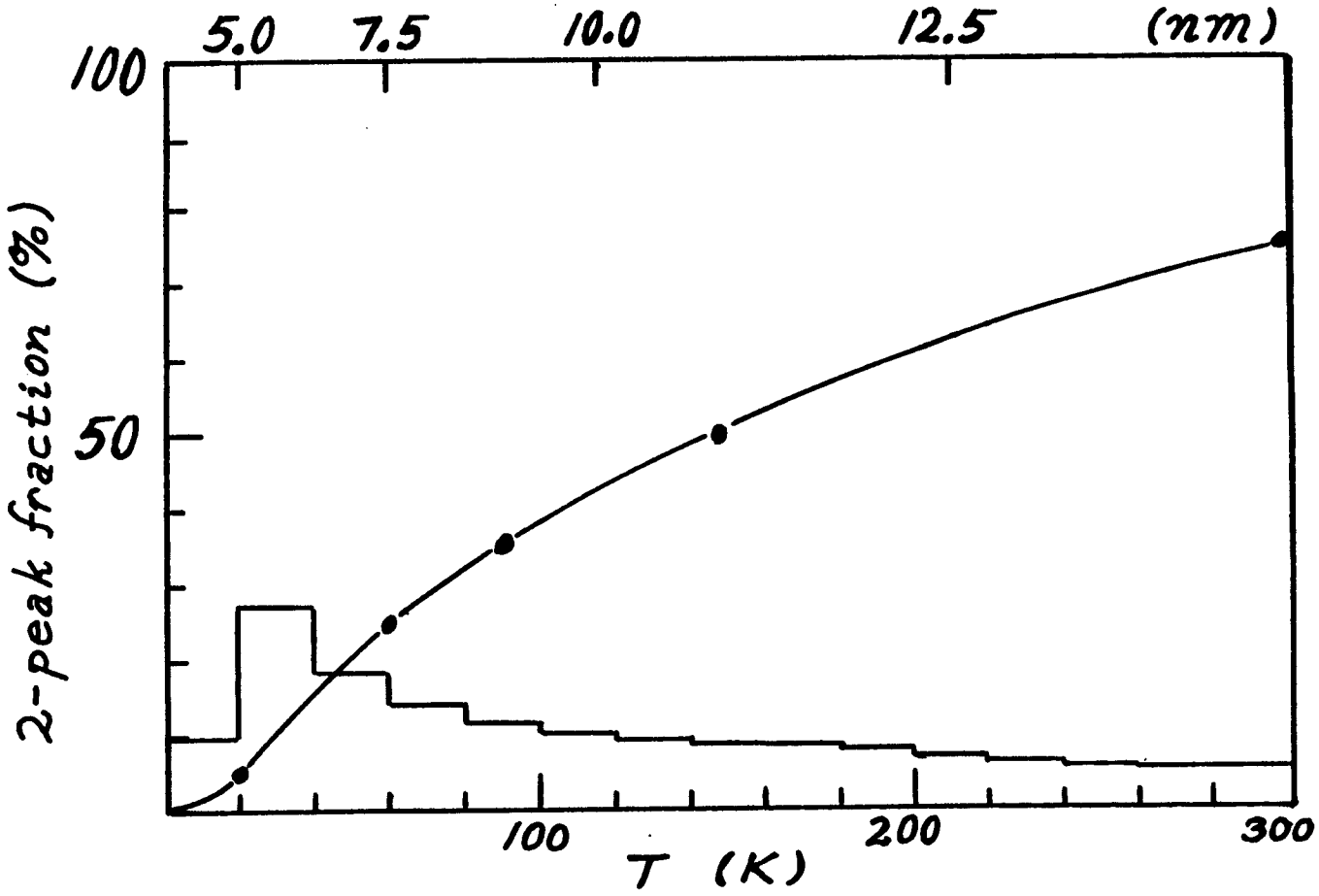

Figure 4. Fractional areas of the 2-peak paramagnetic component of the spectra of Figure 3 as function of temperature. The histogram is obtained by taking, every 20K, the vertical difference in the curve drawn through the fractional areas; it represents a volume distribution, and is calibrated with Equation (2) of the text to give a distribution of diameters of equal-volume spheres (upper scale).

```
        STARTING A NEW FIT . . .  Date:  8/20/86      Time:  1:32:18 PM
-------------------------------------------------------------------------
Data file name... 000206.dat                Data pts...  512   Half (1or2).... 1
Describe experiment.....
Describe the fit........
Peak to peak vel...    7.6500               Overflow...    .0   Output file... F
PSAME... F   YSAME... F   RANDOM.. F   NOSUM... T   NOFIT... T   NTCYC...  15
No. of indep peaks.....  0                  No. sites in hf model..  2
-------------------------------------------------------------------------
     Parameter values:
Background, B......     .5907
   Area, AREA......    7.9716       Parab background corr., GEOM...      .0000
Rel site areas.....     1.0000     1.0000
 center shifts, CS.....    .2600     .4500
   quad params, QQ.....   1.4800    4.8600
   mag. params, GH.....    .0000     .0000
g-exc / g-gnd, GOVG.....   .0000
  equal widths, W.......   .5000
Fixed params....... DEAD   DEAD   DEAD   DEAD   DEAD   DEAD   DEAD   DEAD

        STARTING A NEW FIT . . .  Date:  8/20/86      Time:  1:26:29 PM
-------------------------------------------------------------------------
Data file name... 000206.dat                Data pts...  512   Half (1or2).... 1
Describe experiment.....
Describe the fit........
Peak to peak vel...    7.6500               Overflow...    .0   Output file... F
PSAME... F   YSAME... F   RANDOM.. F   NOSUM... T   NOFIT... T   NTCYC...  15
No. of indep peaks.....  2                  No. sites in hf model..  0
-------------------------------------------------------------------------
     Parameter values:
Background, B......     .5907
   Area, AREA......    7.9716       Parab background corr., GEOM...      .0000
Peak positions, EV.....   -.1480      .6090
    rel. areas, HV.....    .5120      .4880
   half-widths, WV.....    .6930      .6420
 fraction Gau., FGAU....   .0000      .0000
  equal widths, W.......   .0000
Fixed params....... AREA   DEAD   DEAD   DEAD   DEAD   DEAD   DEAD   DEAD

        STARTING A NEW FIT . . .  Date:  8/20/86      Time:  1:21:24 PM
-------------------------------------------------------------------------
Data file name... 000206.dat                Data pts...  512   Half (1or2).... 1
Describe experiment.....
Describe the fit........
Peak to peak vel...    7.6500               Overflow...    .0   Output file... F
PSAME... F   YSAME... T   RANDOM.. F   NOSUM... T   NOFIT... T   NTCYC...  15
No. of indep peaks.....  4                  No. sites in hf model..  0
-------------------------------------------------------------------------
     Parameter values:
Background, B......     .5907
   Area, AREA......    7.9200       Parab background corr., GEOM...      .0000
Peak positions, EV.....   -.1100      .6300    -.7700    1.6600
    rel. areas, HV.....    .4000      .4000     .0500     .0500
   half-widths, WV.....    .5000      .5000     .5000     .5000
 fraction Gau., FGAU....   .0000      .0000     .0000     .0000
  equal widths, W.......   .0000
Fixed params....... AREA   DEAD   DEAD   DEAD   DEAD   DEAD   DEAD   DEAD
```

Figure 5. Examples of screen input to the program. The screens re-form as shown in response to entries for "No. of indep peaks" and "No. of sites in hf model."

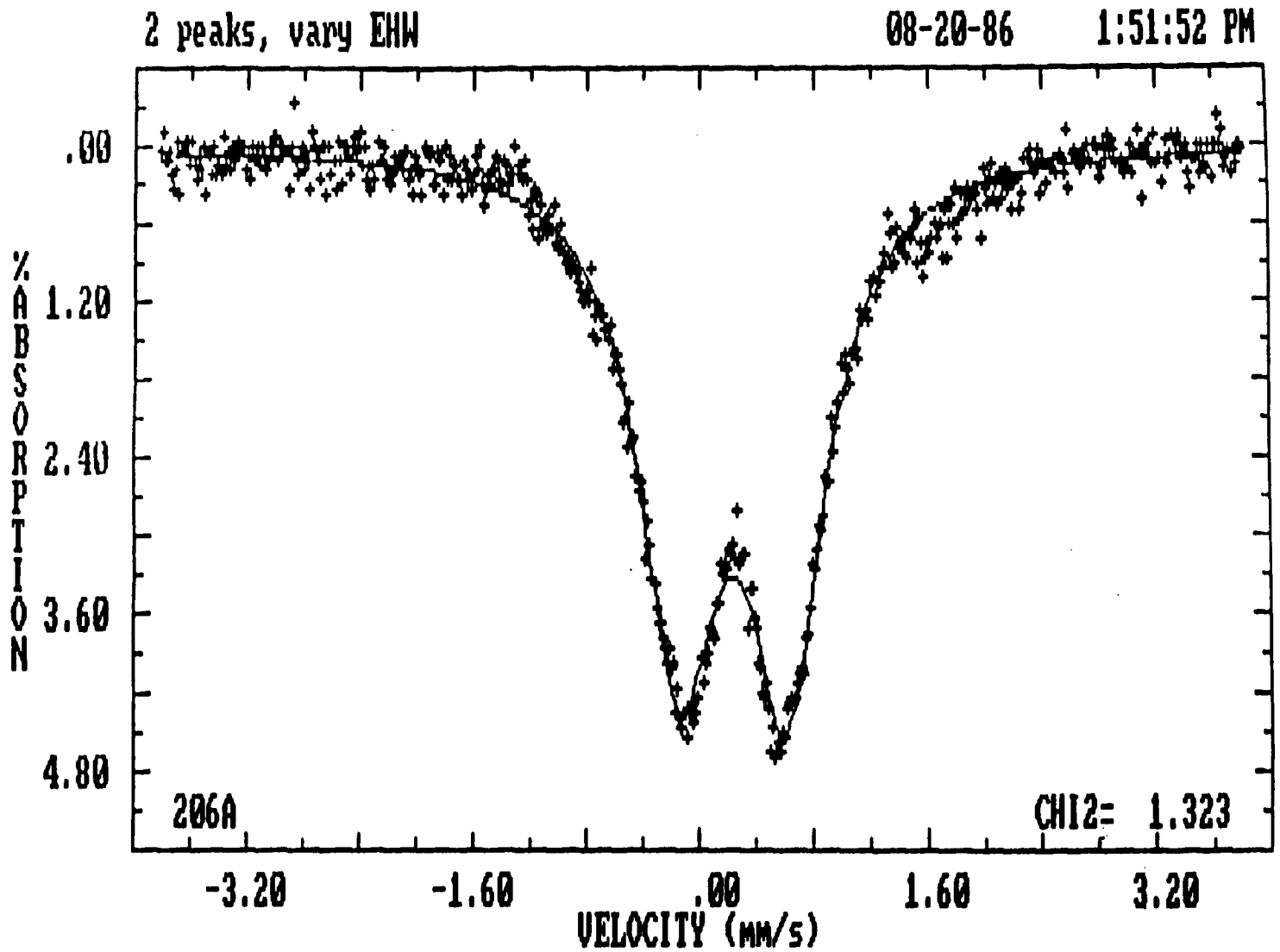

Figure 6. Plot of data and fitted function, as output by VersiFit. The data are from a sample of Fe_2O_3 (7.61 wt%) in 6-nm silica gel.

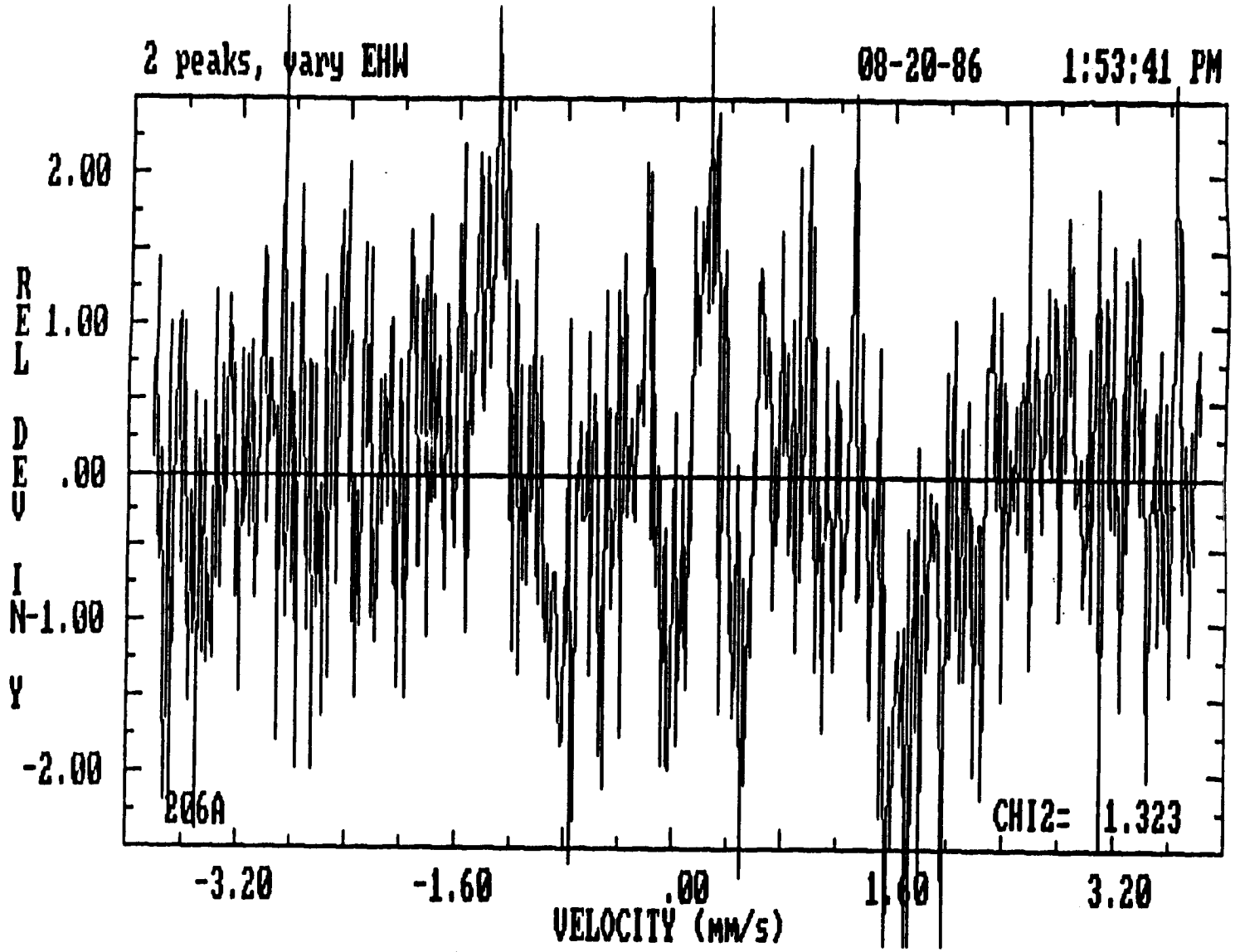

Figure 7. Relative deviation of the data and the fitted function of Figure 6, defined by:

$$r_i = \frac{(y_i - f_i)}{\sigma_i} = \frac{(y_i - f_i)}{y_i}$$

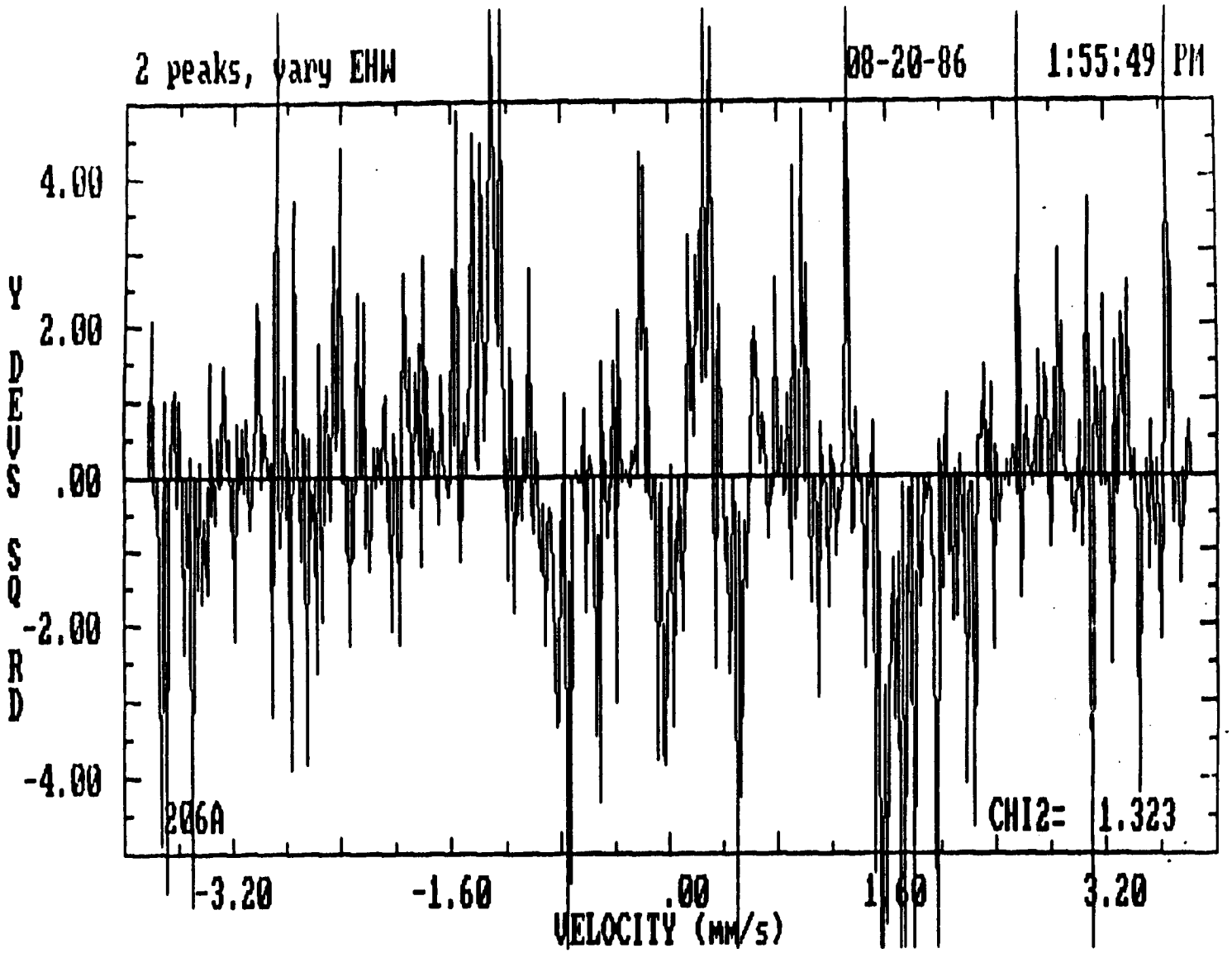

Figure 8. Squares of the values plotted in Figure 7. These are the terms in the sum for χ^2 [Equation (3)].

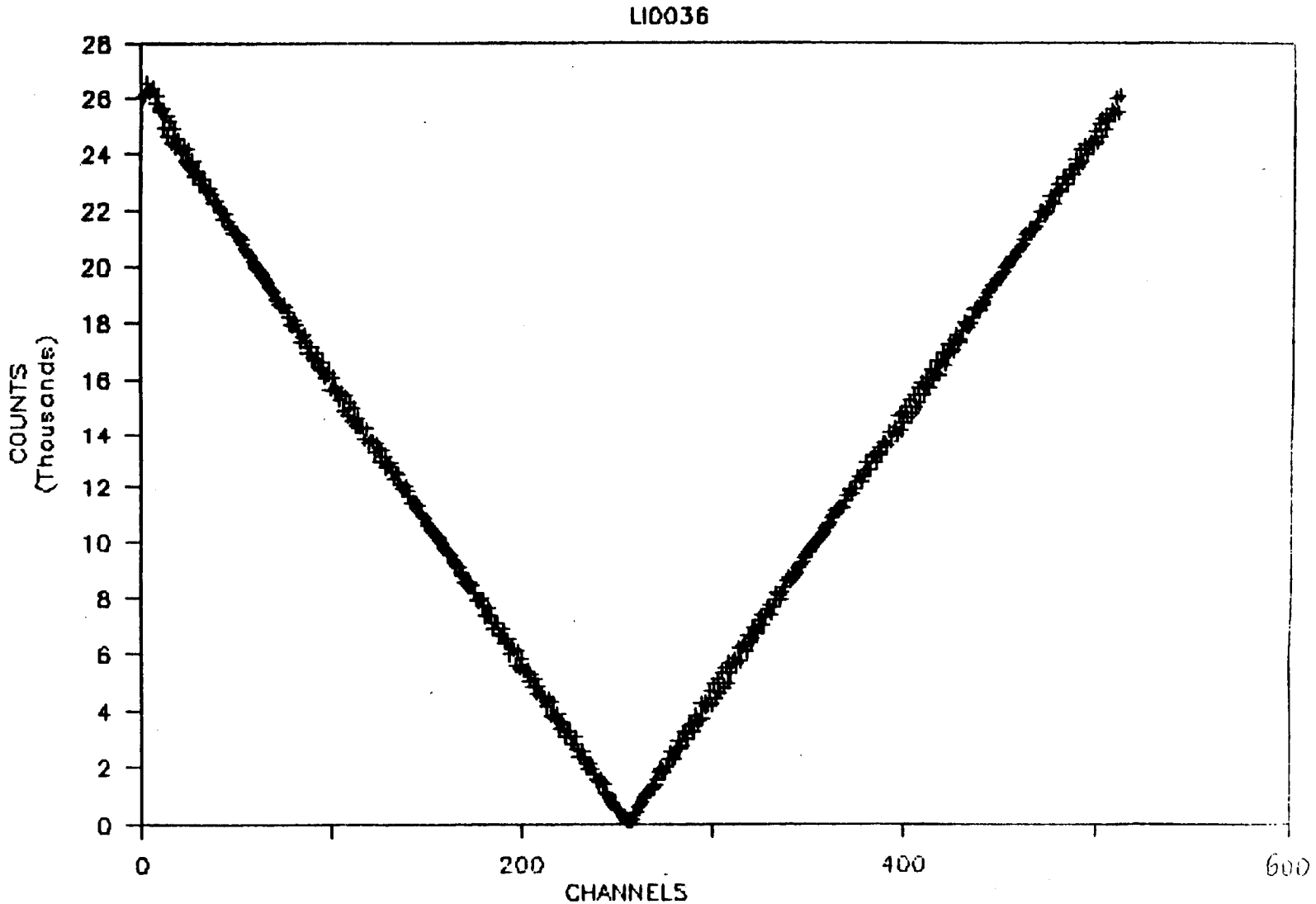

Figure 9. Laser calibration data associated with the spectra of Figures 1,2,11,12.

Iteration	χ^2 by Taylor's	χ^2 by Marquardt
Start	1.126	1.126
1	1.114	1.054
2	1.103	1.010
3	1.094	0.997
4	1.086	0.990
5	1.079	0.987
6	1.072	0.985

Iteration	χ^2 by Taylor's	χ^2 by Marquardt
Start	32.622	32.621
1	18.319	5.833
2	9.957	4.676
3	5.847	1.333
4	1.508	1.240
5	1.483	1.078
6	1.566	1.051
7	1.555	1.023
8	1.541	1.021

Figure 10. Variation of χ^2 for the first few iterations in fitting 6 peaks to the data of Figure 6 by Taylor's or Marquardt procedure. In the upper table, the fit was started relatively close to the minimum of 0.966. In the lower table, the fit was started farther away from the minimum.

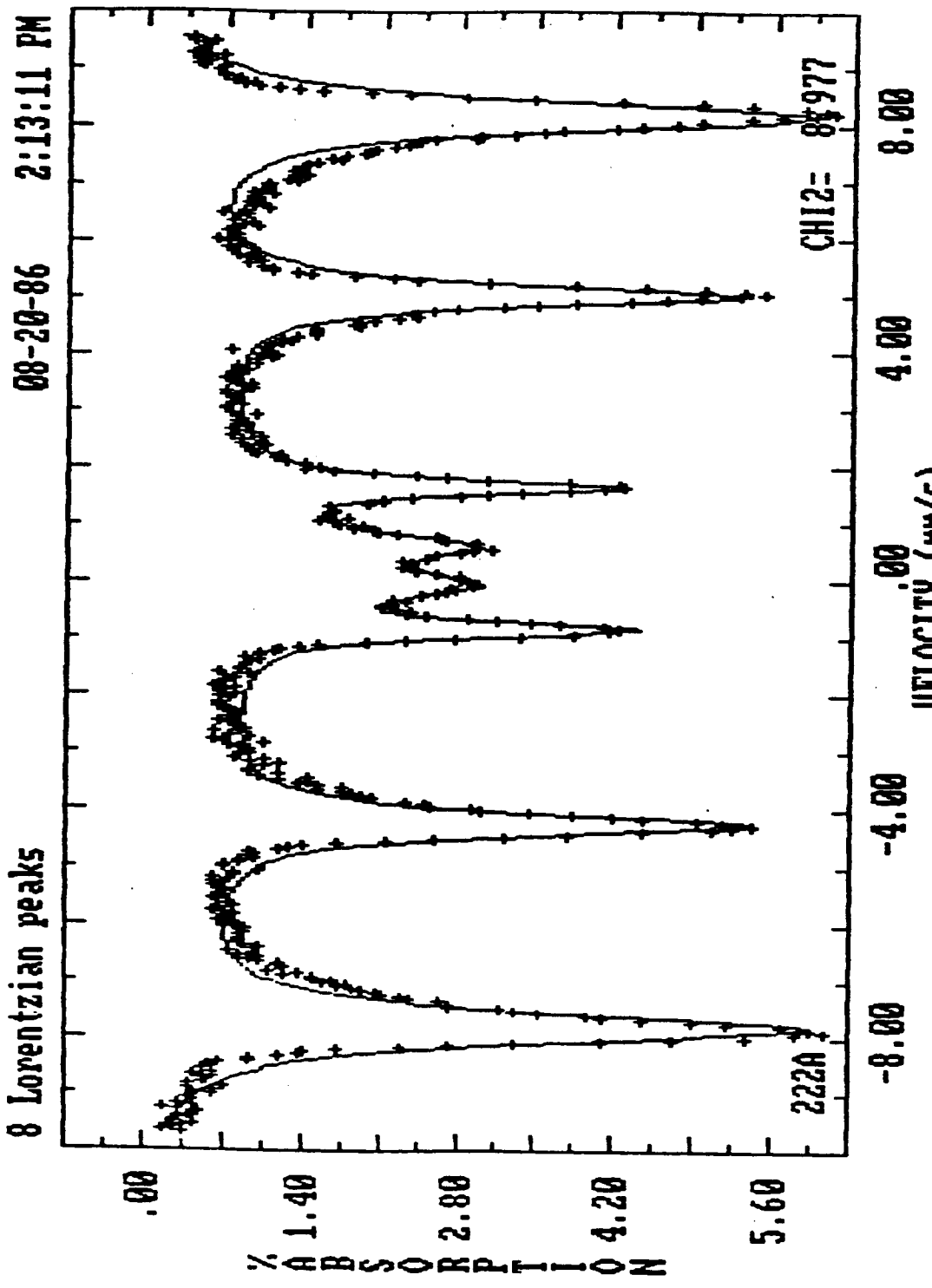

Figure 11. Data of Figure 2 fit to 8 Lorentzian peaks with areas and widths constrained in pairs.

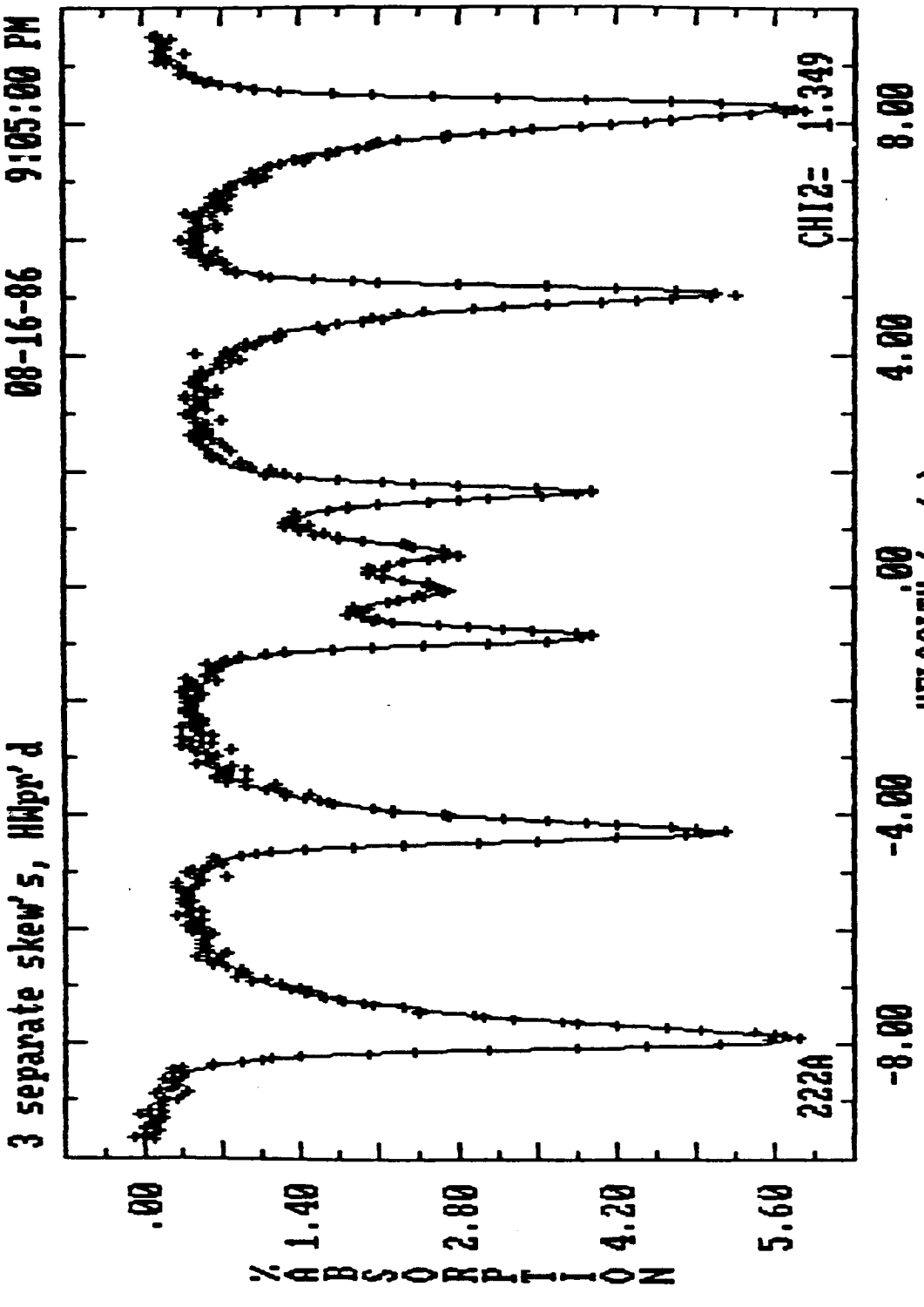

Figure 12. Fit as in Figure 11 with 3 additional "skew" parameters for the 6 magnetic peaks.